CHAPTER 9

STRUCTURAL AND THERMOMICROSCOPIC STUDIES OF *cis*-$Mo(CO)_4(PR_3)_2$ (R= Ph, *m*-tolyl)

9.1 Introduction

As described in chapter 7, the complexes *cis*-$Mo(CO)_4(PR_3)_2$ (R= Ph, *m*-tolyl) have been found to undergo isomerisation in the solid state (scheme 17)

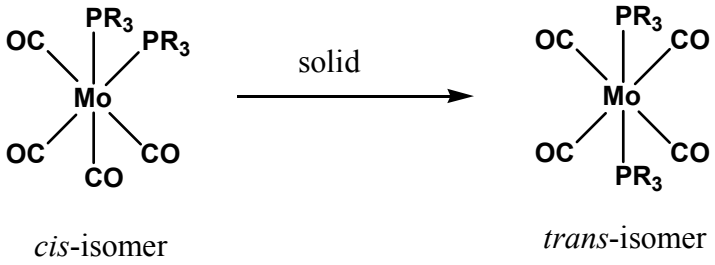

cis-isomer *trans*-isomer

Scheme 17

The mechanism of this solid state rearrangement is not known and hence structural studies on the two complexes were done with a view that the crystallographic information obtained might give an insight into factors that are likely to be responsible for the isomerisation process in the solid state. Interestingly, the complex *cis*-$Mo(CO)_4\{P(m\text{-tolyl})_3\}_2$ has not been prepared before and therefore its crystal structure is reported for the first time [1 -12].

9.2 Experimental

9.2.1 Structural Studies

The complexes (R = Ph and *m*-tolyl) were prepared as in Chapter 7. The crystals of the two complexes were prepared by dissolving the complex (0.5 g) in a minimum amount of dichloromethane (20 ml). An equal amount of ethanol was added slowly to the solution and the samples were stored at -4 ^oC. Yellow crystals of varying sizes developed within three days. These were filtered and dried under a flow of nitrogen. Suitable crystals were selected with the help of an optical microscope and then prepared for mounting on to the diffractometer.

The reflection data of these complexes were collected and structural solution as well as refinement were done as in Chapter 6. The crystal and structural refinement data is shown in Tables 9.1 and 9.3 respectively.

9.2.2 Thermomicroscopic Studies of *cis*-$Mo(CO)_4(P\text{-}m\text{-}tolyl_3)_2$

Optical microscopy experiments were carried out by a slightly modified procedure to that reported previously [13-16]. Single crystals up to 0.5 mm in dimension were used and reactions were performed in an inert atmosphere in the specially constructed cell made out of an aluminium block (see Figure 9.1). The aluminium block is connected to a thermostat. Reactions were performed in the range 130–140 ^{o}C. A CCD camera attachment, fitted to an Olympus polarising microscope, was used to take micrographs of the solid-state isomerisation reaction. The microscope was adjusted for optimum light transmission through an unreacted crystal. Calibration of the equipment was performed with samples of known melting points.

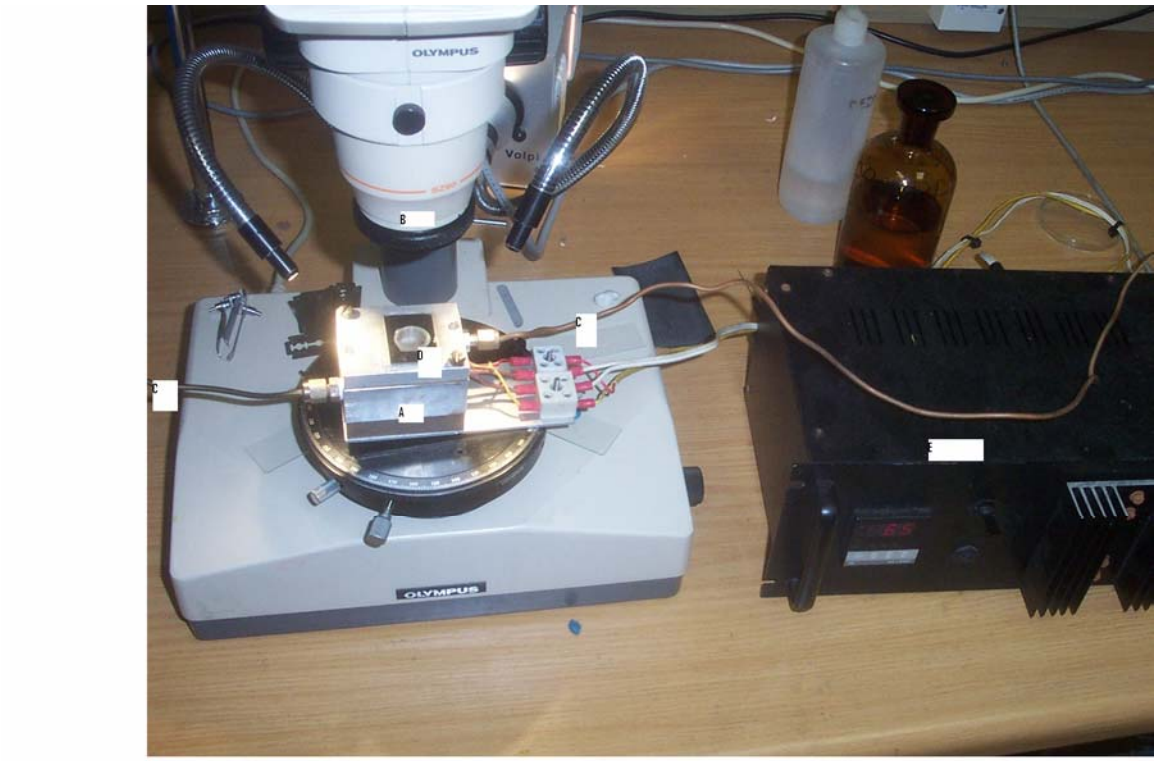

Figure 9.1: Set-up for thermomicroscopic studies: A; aluminium block, B; Olympus polarising microscope with a CCD camera attachemnt, C; nitrogen gas line, D; glass window for aluminium block, E; thermostat

9.3 Results and Discussion

9.3.1 Structural Studies

Molecular structure of *cis*-$Mo(CO)_4(PPh_3)_2$

The molecular structure of the *cis*-$Mo(CO)_4(PPh_3)_2$ is shown in Figure 9.2 as an ORTEP diagram. The hydrogen atoms have been omitted for clarity. The relevant bond distances and angles based on the atomic numbering scheme are listed on Table 9.2. The structure of this complex has been previously studied [6]. The bond lengths and angles found in this study are similar to those reported previously; the slight differences are associated with diffractometers and crystals used.

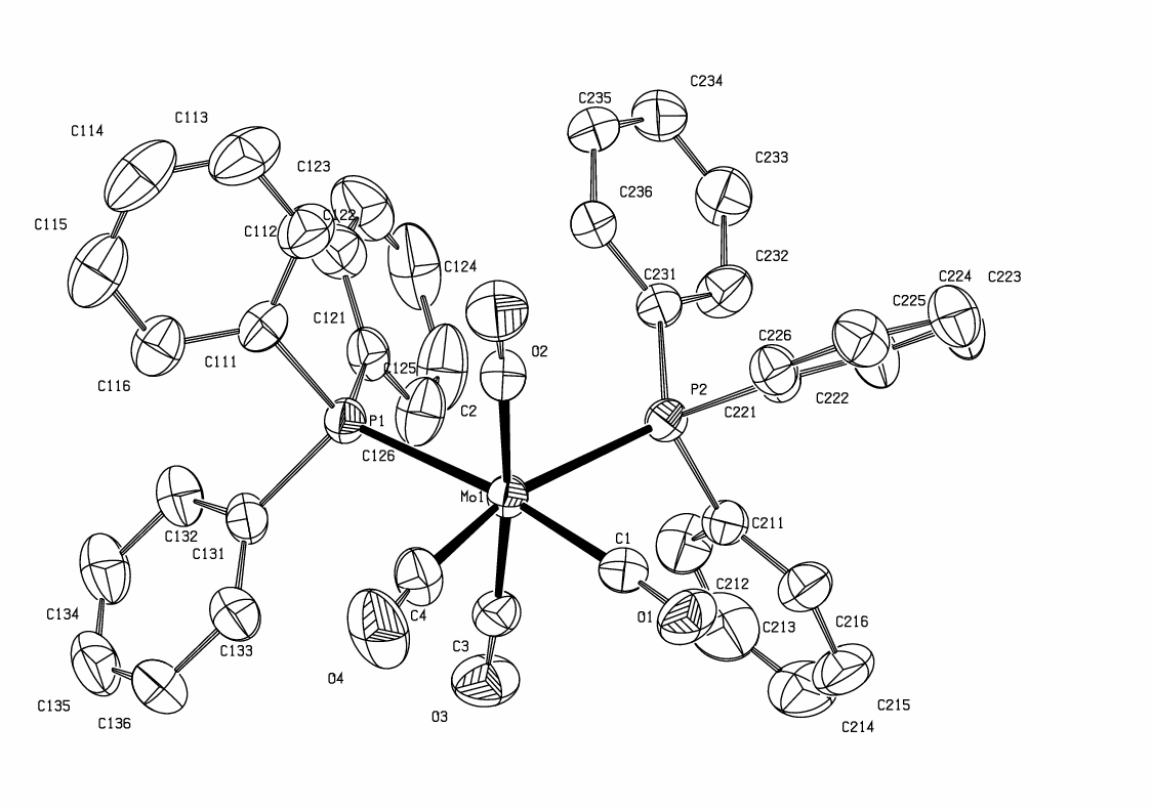

Figure 9.2: ORTEP structure of *cis*-$Mo(CO)_4(PPh_3)_2$ at 50 % probability.

The Mo-P bond lengths are 2.584 (8) and 2.577 (11) Å and the previously studied ones are 2.576(2) and 2.577 (2) Å respectively. The P-Mo-P angle is 104.68 (3)^o and the reported value is 104.62 (7) ^{o}. This angle represents a great distortion from the idealized octahedral geometry. The effect of this distortion is manifested in the geometry of the $Mo(CO)_4$ moiety. The P2-Mo-C4 angle of 163.26(6) [*lit value*163.7(2) ^{o}] and the P2-Mo-C1 of 80.52(6) ^{o} [*lit value* 80.6(2) ^{o}] are direct consequences of the large P-Mo-P dimension. The angle between mutually *cis* CO ligands is 84.53(5) ^{o} and that between mutually *trans* CO ligands is 173.36(5) ^{o}. These are also similar to the observed literature values [6].

The Mo-C distances *trans* to the Mo-P bonds are nearly the same (1.997 (18) and 1.979 (2) Å) and this compares very well with the average literature value of 1.972 (7) Å reported previously

The other Mo-C bond distances are 2.062 and 2.021 Å [lit values 2.059 (9) and 2.022 (9)]. All the other bond lengths and angle in the phosphine ligands are normal.

Table 9.1: Crystal data and structure refinement for *cis*-$Mo(CO)_4(PPh_3)_2$

Chemical Formula	$C_{40}H_{30}MoO_4P_2$
Formula weight	732.52
Temperature/K	293 (2)
Wavelength/Å	0.71073
Crystal System	triclinic
Space group	P-1
a/ Å	9.647(5)
b/ Å	11.543(5)
c/ Å	16.938(5)
α/^{o}	99.974(5)
β/ ^{o}	98.029(5)
γ/ ^{o}	110.243(5)
Volume/ Å^3	1701.7(13)
Z	2
Density (calculated)/g.cm^{-3}	1.430
Absorption coefficient/ mm^{-1}	0.520
F(000)	748
Crystal size/mm	0.37 x 0.34 x 0.30
Theta range/^{o}	1.94 to 28.30
Index range	-12<=h<=12, -15<=k<=14, -18<=l<=22
Reflections collected	11773
Independent reflections	8161 [R(int) = 0.0209]
Completeness to theta = 28.00^o	96.4 %
Refinement method	Full-matrix least-squares on F^2
Data/restraints/parameters	8161 / 0 / 424
Goodness - of –fit on F^2	1.034
Final R indices [I>2σ(I)]	R1 = 0.0254, wR2 = 0.0639
R indices (all data)	R1 = 0.0294, wR2 = 0.0661
Largest diff.peak	0.248
And hole/ e$^-$/ Å^{-3}	-0.513 e.Å^{-3}

Table 9.2: Important bond distances ($Å^3$) and bond angles(^{o}) for *cis*-$Mo(CO)_4(PPh_3)_2$

Mo-P1	2.5837(8)	P2-Mo-C1	80.52(6)	Mo-C1-O1	176.66(15)
Mo-P2	2.5766(11)	P2-Mo-C2	93.94(5)	Mo-C2-O2	176.69(16)
Mo-C1	1.9927(18)	P2-Mo-C3	89.96(5)	Mo-C3-O3	176.72(16)
Mo-C2	2.0621(18)	P2-Mo-C4	163.26(6)	Mo-C4-O4	171.40(18)
Mo-C3	2.0209(18)	C1-Mo-C2	93.18(7)	P1-C111-C112	119.33(15)
Mo-C4	1.979(2)	C1-Mo-C3	91.42(7)	P1-C111-C116	122.46(15)
C1-O1	1.147(2)	C1-Mo-C4	82.74(8)	P1-C121-122	125.04(15)
C2-O2	1.141(2)	C2-Mo-C3	174.40(7)	P1-C121-126	116.52(15)
C3-O3	1.148(2)	C2-Mo-C4	86.97(8)	P1-C131-C133	121.69(14)
C4-O4	1.152(2)	C3-Mo-C4	90.45(8)	P1-C131-C132	120.23(14)
P1-C111	1.8353(18)	Mo-P1-C111	117.70(6)	P2-C211-C212	120.30(14)
P1-C121	1.8444(18)	Mo-P1-C121	116.98(6)	P2-C211-C216	121.07(13)
P1-C131	1.8508(17)	Mo-P1-C131	115.44(7)	P2-C221-C222	119.44(13)
P2-C211	1.8367(16)	C111-P1-C121	103.05(9)	P2-C221-C226	122.55(13)
P2-C221	1.8465(16)	C111-P1-C131	101.89(8)	P2-C231-C232	123.84(13)
P2-C231	1.8365(18)	C121-P1-C131	99.01(8)	P2-C231-C236	116.93(13)
P1-Mo-P2	104.68(3)	Mo-P2-C211	109.70(6)		
P1-Mo-C1	173.36(5)	Mo-P2-C221	116.23(6)		
P1-Mo-C2	90.59(6)	Mo-P2-C231	124.09(5)		
P1-Mo-C3	84.53(5)	C211-P2-C221	101.59(8)		
P1-Mo-C4	92.01(6)	C211-P2-C231	98.71(8)		

Crystal Structure

The complex *cis*-$Mo(CO)_4(PPh_3)_2$ crystallizes in the triclinic space group P-1 as previously observed. There are two molecules per unit cell (Figure 9.3). The molecules pack in 'ABAB' layers (Figure 9.4). As seen from the diagram, the PPh_3 ligands of one molecule in a row face the PPh_3 ligands of the next molecule in the same row and this tends to cause greater repulsion and hence instability within the crystal lattice. There are voids within the crystal lattice and, this therefore suggests that they may provide reaction cavities within the structure which allows for isomerisation to take place. These cavities therefore allow flexing of the phosphine ligands during heating and hence conversion to a more stable isomer *trans*-$Mo(CO)_4(PPh_3)_2$.

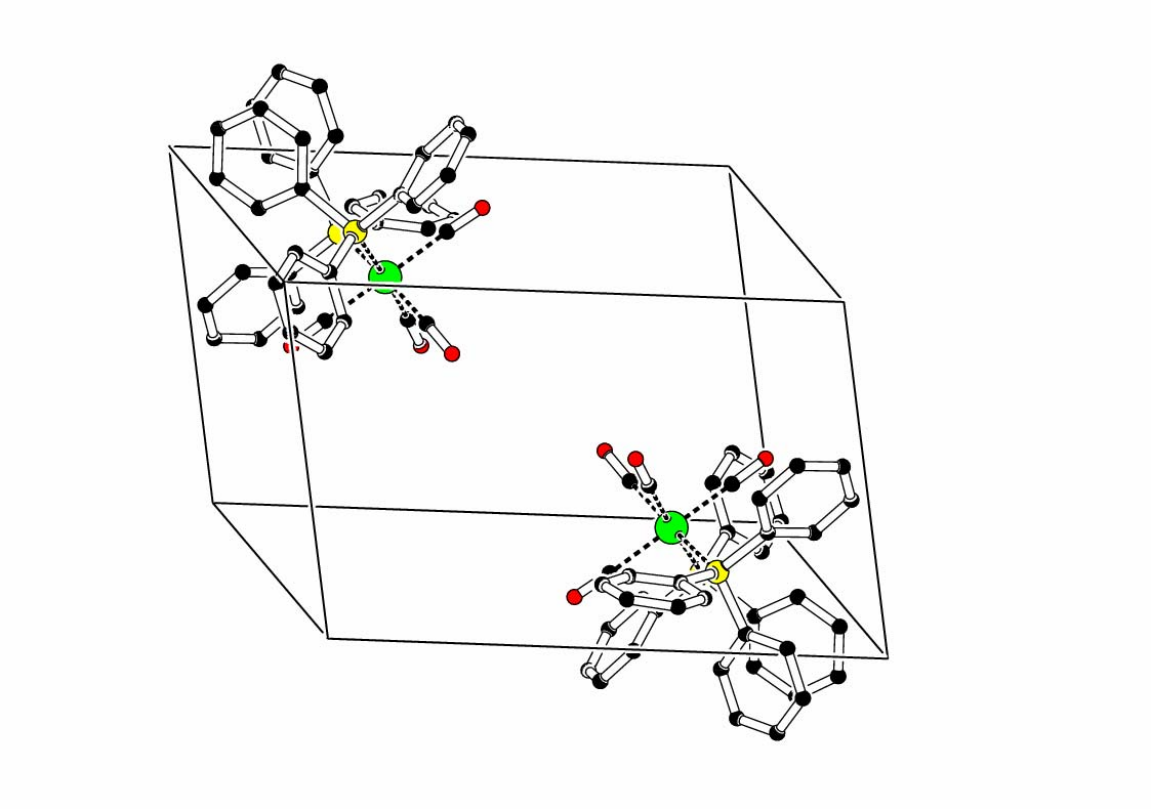

Figure 9.3: Unit cell of *cis*-$Mo(CO)_4(PPh_3)_2$ (hydrogen atoms omitted for clarity)

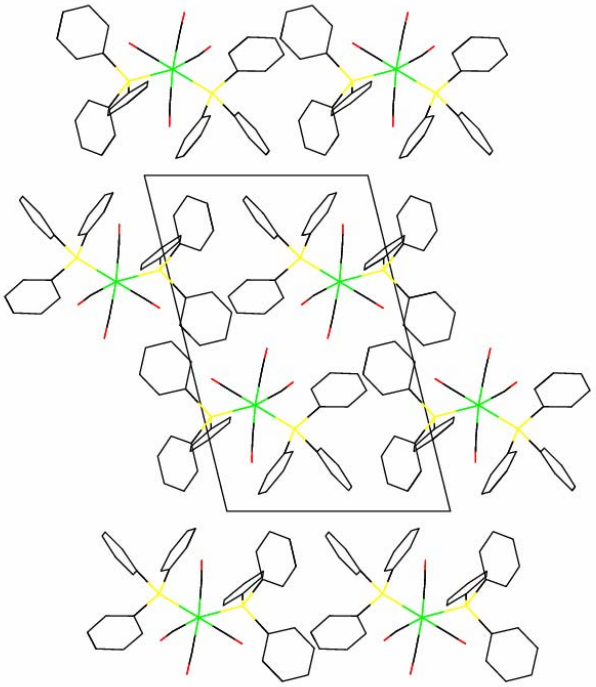

Figure 9.4: Extended packing diagram of *cis*-$Mo(CO)_4(PPh_3)_2$ molecules in xo plane.

The molecular structure of *cis*-$Mo(CO)_4\{P(m\text{-tolyl})\}_2$

Crystal and structural refinement data for *cis*-$Mo(CO)_4\{P(m\text{-tolyl})\}_2$ are shown in Table 9.3.

Table 9.3: Crystal and Refinement Data of *cis*-$Mo(CO)_4\{P(m\text{-tolyl})\}_2$

Crystal and Refinement Data	
Chemical formula $C_{46}H_{42}O_4P_2Mo$ Formula weight = 816.68 Monoclinic $P2_1/n$ a = 10.971(5) Å b = 19.504(5) Å c = 19.037(5) Å $\beta = 90.715(5)^o$ V = 4073(2) $Å^3$ Z = 4 Density (calculated) = 1.3318 g cm^{-3} Wavelength (Mo Kα) = 0.71073Å Absorption coefficient μ= 0.442 mm^{-1} F (000) = 1688 Crystal size = 0.5mm x 0.48mm x 0.38mm	Theta range = 1.49 to 28.29^o Index range = -14≤h≤14, -25≤k≤25,-25≤l≤15 Reflections collected = 28139 Independent reflections = 10047(Rint) =).681 Data/restraints/parameters = 10047/0/478 Goodness of Fit on F^2 = 0.937 Final R indices (I>2σ(I) = 0.0382 R indices (all data) = 0.669 Largest diff. peak and hole/e-/ $Å^3$ = 0.6300/ -0.500

The molecular structure of *cis*-$Mo(CO)_4\{P(m\text{-tolyl})\}_2$ is illustrated in Figure 9.5 as an ORTEP diagram. Hydrogen atoms have been omitted for clarity. The relative bond distances and bond angles based on the atomic numbering scheme in this figure are listed in table 9.4

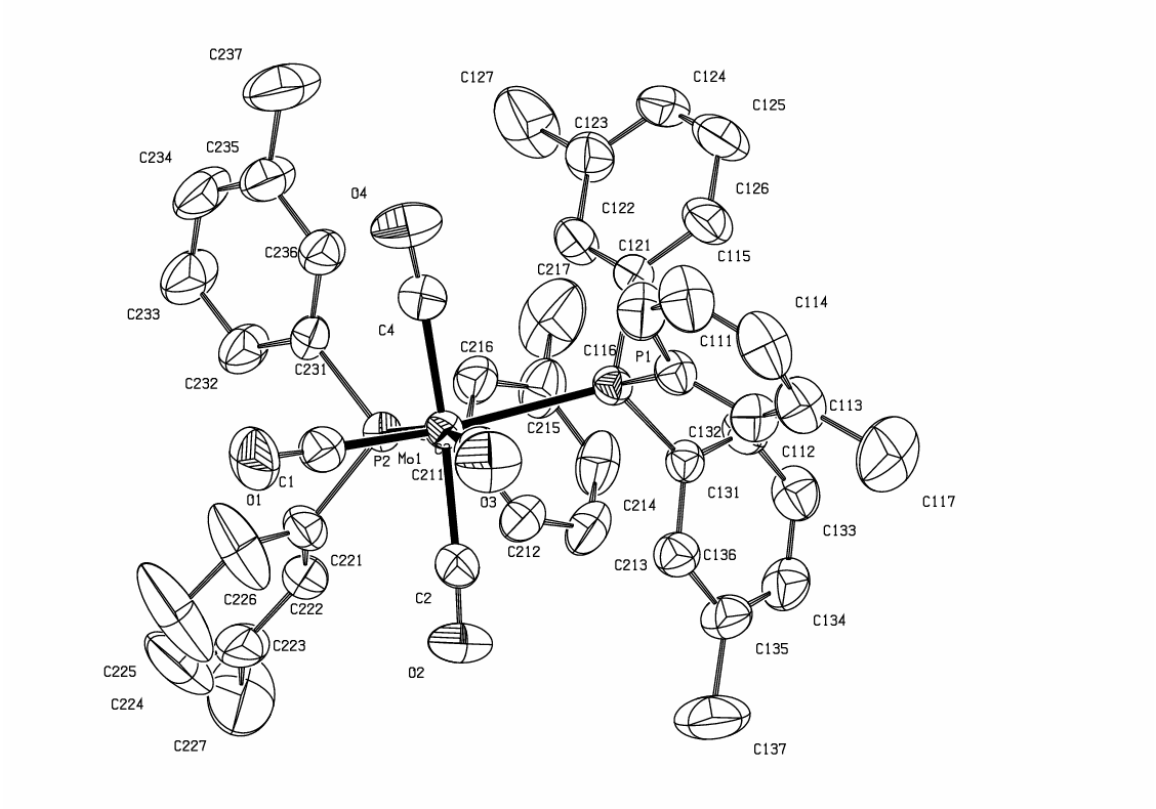

Figure 9.5: ORTEP with thermal ellipsoids drawn at 50 % probability

As seen from Figure 9.5, the complex adopts the typical octahedral geometry of six coordinate complexes. Some distortion from a regular geometry as observed with the molecular structure of L = PPh_3 is noted in the P1-Mo-P2 bond angle, which is also large at 100.51^o but not as large as that of L = PPh_3. This is a result primarily obtained from the accommodation of a sterically congested environment brought about by the bulky tri-*m*-tolylphosphine ligands. The same distortion has been noted in other complexes of the type *cis*-$Mo(CO)_4(PR_3)_2$ [7]. The two Mo-P bond distances are nearly the same at 2.6049(13) and 2.6106(13) Å. They are slightly different from the ones observed in the literature (see Table 9.6). The *cis*-$Mo(CO)_4\{P(m\text{-tolyl})\}_2$ is sterically crowded when compared to most of the other complexes shown in table 9.5 and thus the increase in Mo-P distance may be a direct response to this bulkiness of the *m*-tolylphosphine ligand. Thus when the phosphines

move further apart from the metal centre, the steric repulsion between the two phosphines is reduced.

There are two different sets of carbonyl ligands seen in the structure. The carbonyl ligands *trans* to the *m*-tolylphosphine ligands are closer to the metal centre with Mo-C bond distances of 1.964(3) and 1.978(3) Å while the CO ligands *cis* to the phosphines are bound at 2.039(3) and 2.025(3) Å. The same applies to the C-O bond distances of 1.155(3), 1.150(3) Å and 1.143(4), 1.149(3) respectively. The steric interaction between the two phosphine ligands tends to affect the $Mo(CO)_4$ moiety as observed with L = PPh_3. The C1-Mo-C3 bond angle of 81.68(11)^o deviates from the normal angle of 90^o. This is observed for other complexes previously studied. The other bond distances are normal. Large thermal ellipsoids are observed for the methyl groups on the phosphine groups and a few carbons in the phenyl ring. This implies large disorder in phosphine ligands and therefore during heating the phenyl rings could easily shift to a *trans* position on isomerisation.

The crystal structure of *cis*-$Mo(CO)_4${P(*m*-tolyl)}$_2$

The *cis*-$Mo(CO)_4${P(*m*-tolyl)}$_2$ complex crystallize in the monoclinic space group $P2_1/n$ (Table 9.3). This space group has been observed for other molybdenum complexes of this type; the other typical space group is $P_{21/c}$ [1-12].

The crystal structure of *cis*-$Mo(CO)_4${P(*m*-tolyl)}$_2$ and its extended packing diagram are shown in Figures 9.6 and 9.7 respectively. There are four molecules of the complex per unit cell. The extended packing diagram shows that the molecules pack in 'ABAB'-type layers with the two CO ligands *trans* to the phosphine ligands from one molecule pointing towards one of the two phosphine ligands in the molecule next to it. The phosphine ligands in one layer are staggered with respect to other phosphine ligands in the next layer. The packing arrangement is well suited for the bulky tri-*m*-tolylphosphine ligands. There seem to be channels between the four molecules within one unit cell involving two phosphine ligands and two CO ligands. Possible interactions between the CO of one molecule and one

of the tolyl rings in the next molecule have been observed and this probably stabilizes the crystal structure.

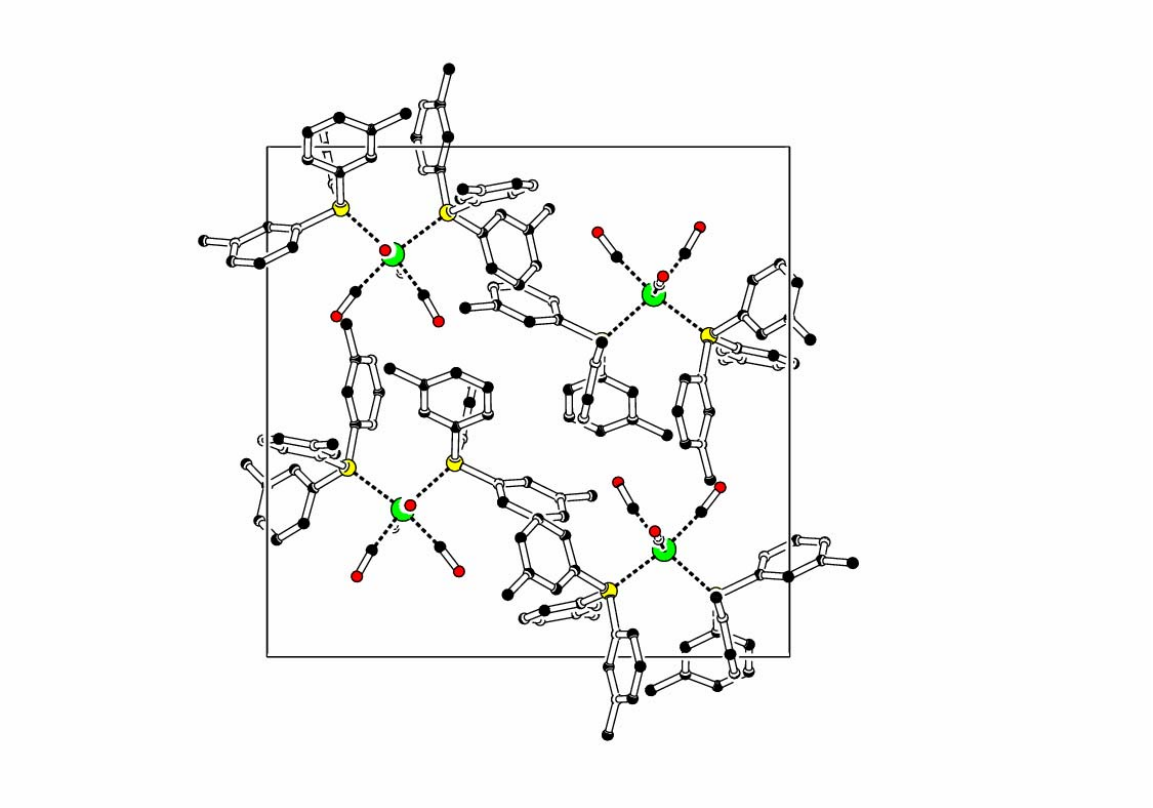

Figure 9.6: Unit cell of *cis*-$Mo(CO)_4\{P(m\text{-tolyl})\}_2$

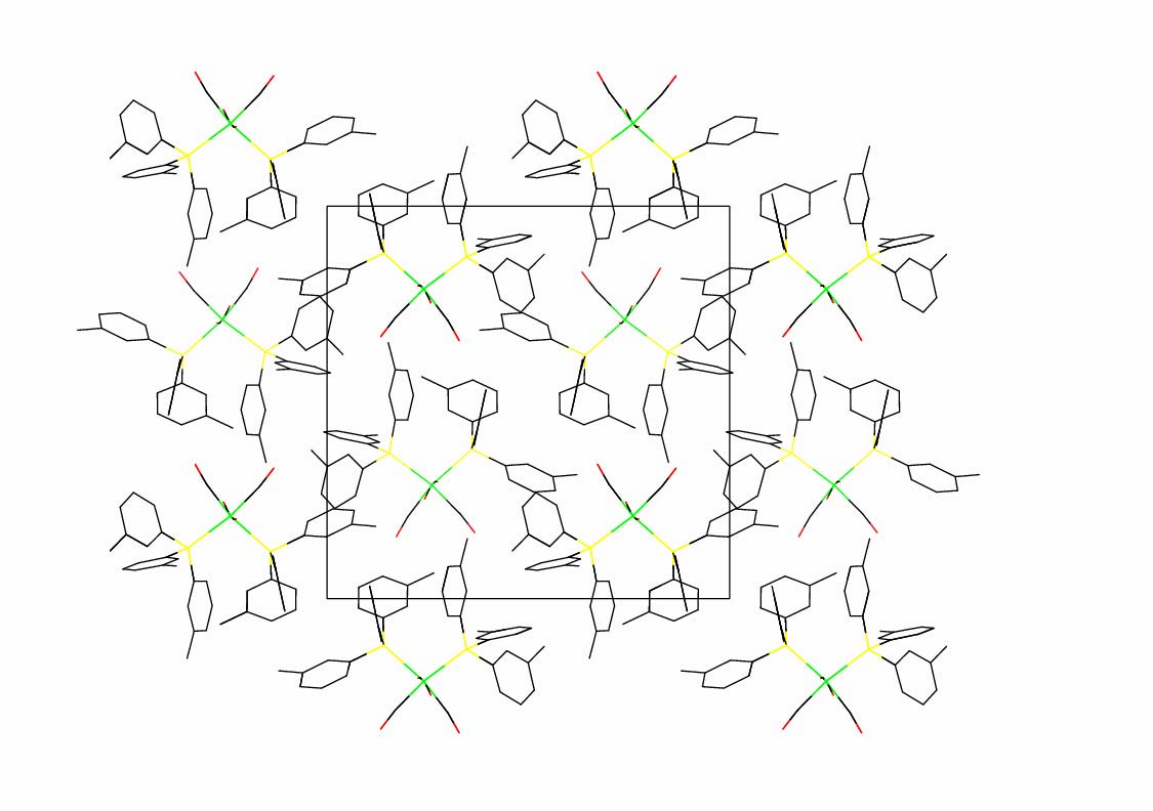

Figure 9.7: Extended packing of *cis*-$Mo(CO)_4\{P(m\text{-tolyl})\}_2$

Table 9.5: Selected bond distances (Å) and Angles (degrees)

Mo-P1	2.6049(13)	P2-Mo-C1	91.37(8)	Mo-C1-O1	172.1(2)
Mo-P2	2.6106(13)	P2-Mo-C2	83.76(7)	Mo-C2-O2	175.5(2)
Mo-C1	1.964(3)	P2-Mo-C3	169.47(7)	Mo-C3-O3	173.0(2)
Mo-C2	2.039(3)	P2-Mo-C4	99.01(7)	Mo-C4-O4	173.6(2)
Mo-C3	1.978(3)	C1-Mo-C2	89.59(10)	P1-C111-C112	124.05(17)
Mo-C4	2.025(2)	C1-Mo-C3	81.68(11)	P1-C111-C116	117.33(19)
C1-O1	1.155(3)	C1-Mo-C4	85.26(10)	P1-C121-122	120.41(17)
C2-O2	1.143(4)	C2-Mo-C3	88.26(10)	P1-C121-126	121.76(18)
C3-O3	1.150(3)	C2-Mo-C4	174.20(10)	P1-C131-C132	123.45(17)
C4-O4	1.149(3)	C3-Mo-C4	88.34(10)	P1-C131-136	118.41(17)
P1-C111	1.846(3)	Mo-P1-C111	111.33(8)	P2-C211-C212	118.32(18)
P1-C121	1.838(2)	Mo-P1-C121	117.06(7)	P2-C211-C216	123.36(17)
P1-C131	1.832(2)	Mo-P1-C131	119.43(7)	P2-C221-C222	123.3(2)
P2-C211	1.834(2)	C111-P1-C121	100.34(10)	P2-C221-C226	118.2(2)
P2-C221	1.847(3)	C111-P1-C131	103.07(10)	P2-C231-C232	122.08(17)
P2-C231	1.844(2)	C121-P1-C131	103.09(10)	P2-C231-C236	119.47(18)
P1-Mo-P2	100.51(2)	Mo-P2-C211	117.37(7)	Mo-C1-O1	172.1(2)
P1-Mo-C1	166.62(8)	Mo-P2-C221	112.49(8)		
P1-Mo-C2	97.73(7)	Mo-P2-C231	118.92(8)		
P1-Mo-C3	87.35(8)	C211-P2-C221	102.25(11)		
P1-Mo-C4	86.80(7)	C211-P2-C231	103.21(10)		

Table 9.6: Comparison of selected bond distances(Å) and angles(^{o}) for *cis*-$Mo(CO)_4(PR_3)_2$ complexes as obtained from reference [7]

	L						
	PMe_3	PEt_3	$P(n\text{-}Bu)_3$	PMe_2Ph	$PMePh_2$	PPh_3	**P(m-tolyl)**
Mo-P(average)	2.522(1)	2.544(4)	2.522(8)	2.529(5)	2.555(14)	2.57(7)	2.61(13)
Mo-C(*trans*)	1.971(6)	1.977(1)	1.96(1)	1.982(3)	1.978(4)	1.972(2)	1.971(3)
Mo-C(*cis*)	2.032(14)	2.032(5)	1.99(1)	2.016(18)	2.027(7)	2.040(19)	2.032(3)
P-Mo-P	97.54(4)	100.27(3)	99.29(9)	94.78(5)	92.52(5)	104.62(7)	100.51(2)
P1-Mo-C1	173.2(2)	172.1(2)	173.0(3)	175.5(2)	178.5(2)	163.7(2)	166.62(8)
P1-Mo-C2	85.0(2)	87.1(1)	86.6(1)	87.1(2)	92.9(2)	80.6(2)	97.73(7)
P2-Mo-C1	89.3(2)	87.4(1)	87.7(3)	89.7(2)	87.8(2)	91.7(2)	91.37(8)
P2-Mo-C2	89.9(2)	91.8(1)	92.8(3)	87.0(2)	95.8(2)	84.4(2)	83.76(7**)**
P1-Mo-C3	90.5(2)	89.5(1)	92.4(3)	89.3(2)	90.6(2)	94.0(2)	87.35(8)
P1-Mo-C4	90.8(1)	86.9(1)	91.1(3)	87.8(2)	88.9(2)	90.3(2)	86.80(7)
P2-Mo-C3	177.4(2)	172.1	173.4	176.3(2)	172.2(2)	173.2(2)	169.47(7)
P2-Mo-C4	88.5(2)	88.6(1)	88.3(3)	94.0(2)	88.8(2)	90.6(2)	99.01(7)

9.3.2 Thermomicroscopic Studies of *cis*-$Mo(CO)_4(P(m\text{-tolyl})_3)_2$

Thermomicroscopic studies were carried out on selected crystals of *cis*-$Mo(CO)_4(P(m\text{-tolyl})_3)_2$ complex at temperatures of 130, 140 and 150 ^oC.

On heating the crystals at 140 ^oC, the surface of the crystals gradually changed from yellow to orange and then to a dark colour (See figure 9.8). When one crystal was cut in half, the crystal shattered and the inner surface was observed to be yellow and only the outer surface was dark (Figure 9.9). Similar colour changes were observed by visual inspection when heating samples in an NMR tube. When the heated crystals were dissolved in $CDCl_3$ and then taken for ^{31}P NMR spectral analysis the sample showed about 10 % conversion to the *trans* isomer (with no other species present). The data shows that the isomerisation reaction is a surface initiated reaction. Heating at 130 ^oC, the colour gradually changed from yellow colour to opaque. After the sample was heated for 4 h, NMR analysis of the sample revealed that it had only undergone slight conversion, less than 5 %. Isomerisation occured without any crystal degradation during heating. However, analysis by single-crystal X-ray diffraction showed that the crystal had lost its crystallinity. Isomerisation at 130 ^oC is very slow. The yellow colour to opaque colour change signified the onset of the isomerisation reaction. The orange colour change observed during the heating could possibly indicate a further transition to a high temperature intermediate phase beginning at the crystal surface.

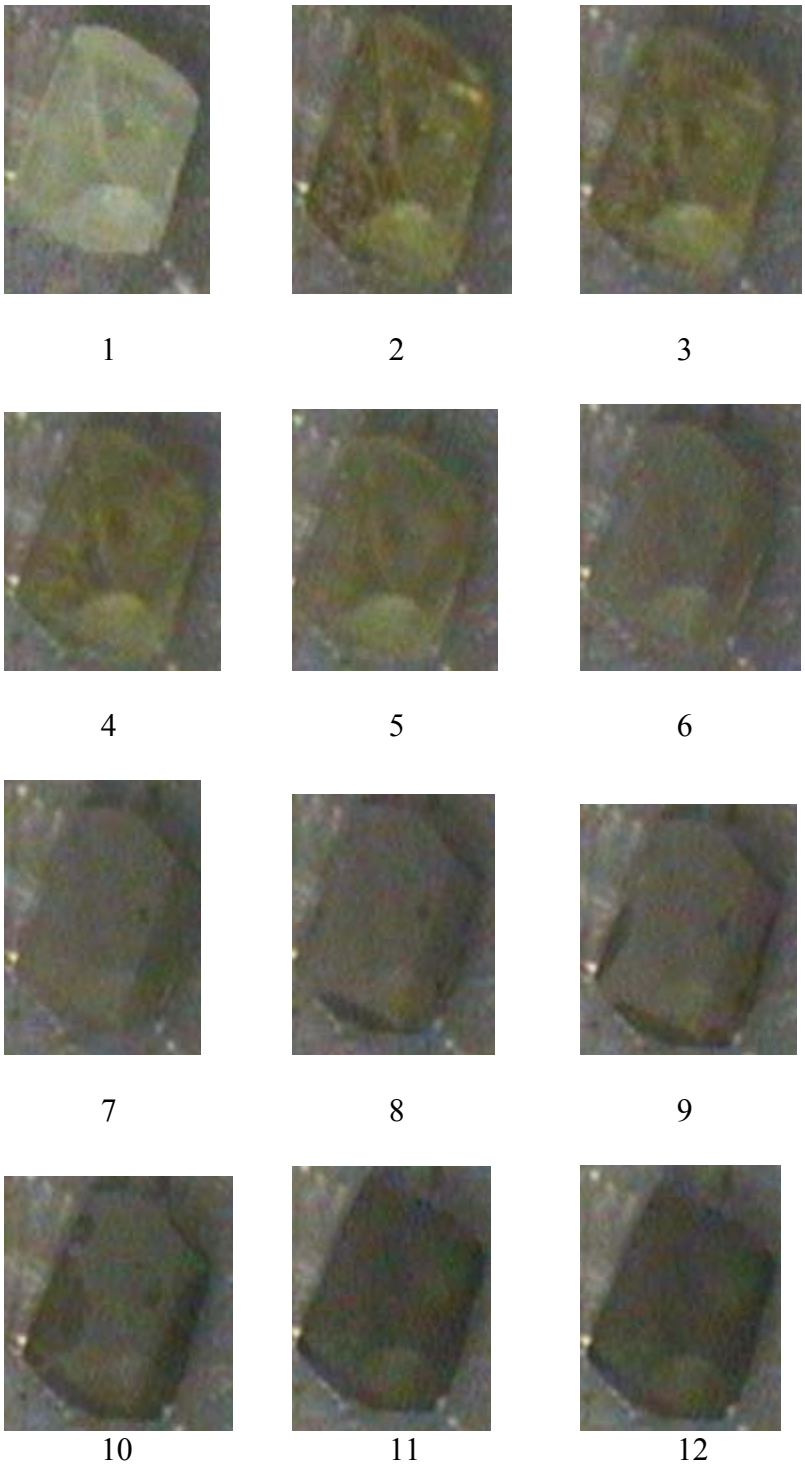

Figure 9.8: Heating *cis*-Mo(CO)4(P-*m*-tolyl$_3$)$_2$ for 2 hours (Pictures taken at 10 minutes interval)

Figure 9.9: Fractured crystal from figure 9.8 (picture 12)

9.4 Conclusion

Structures of *cis*-$Mo(CO)_4(PR_3)_2$ (R = Ph and *m*-tolyl) have been solved with R factors of less than 5 %. The packing arrangements of these complexes have been determined and the results have been used to rationalize the solid state isomerisation process. Thermomicrospic investigations were also carried out and the studies revealed that the isomerisation process is a surface initiated reaction.

9.5 References

1 S. W. Kirtley, Comprehensive Organometallic Chemistry, vol 3, Chapter 27, Pergamon Press, Oxford.

2 M. A. Ardon, P. D. Hayes, G. Hogarth, *J. Chem. Edu.* **79** (2002) 1249.

3 D. J. Darensbourg; R. L. Kump, *Inorg. Chem*. **17** (1978) 2680.

4 D. J. Darensbourg, *Inorg. Chem.* **18** (1979) 14.

5 D. J. Darensbourg; A. H. Graves, *Inorg. Chem.* 18 (1979) 1257.

6 F. A. Cotton; D. J. Darensbourg; S. Klein, B. W. S. Kolthammer, *Inorg. Chem*. **21** (1982) 294.

7 F. A Cotton, D. J. Darensbourg; S. Klein, B. W. S. Kolthammer, *Inorg. Chem*. **21** (1982) 2661 .

8 M. Watson, S. Woodward, G. Conole, M. Kessler, G. Sykara, *Polyhedron* **13** (1994) 2455.

9 J. E. Cortes-Figueroa, M. S. Leon-Velaguez, J. Ramos, J. P. Jasinki, D. A. Keene, J. D. Zubkowski, E. J. Valente, *Acta Cryst*. **C56** (2000) 1435.

10 E.C. Alyea, G. Ferguson, S. Kannan, *Acta Cryst*. **C52** (1996) 765.

11 O. Shawkataly, A. Umuthavan, K. Ramalingam, H-K Fun, A.R. Ibrahim, *Acta Cryst*. **C53** (1997) 1543.

12 E.C. Alyea, G. Ferguson, J. F. Gallagher, S. Song, *Acta Cryst*. **C50** (1994) 1084.

13 R. S. Bogadi, MSc Thesis, University of the Witwatersrand, Johannesburg, 2002.

14 O. M. P. Horwood, MSc Thesis, University of the Witwatersrand, Johannesburg, 2003.

15 R. S. Bogadi, D. C. Levendis and N. J. Coville, *J. Am. Chem. Soc.* **124** (2002) 1104.

16 O. M. P. Horwood, D. G. Billing, D. C. Levendis, F. M. Nareetsile, N. J. Coville, *CrystEngn Commun*, **5** (2003) 468.